ASIAN JOURNAL OF CIVIL ENGINEERING (BHRC) VOL. 15, NO. 6 (2014)
PAGES 803-815

SEISMIC FRAGILITY CURVES FOR MID-RISE RC FRAMES DESIGNED ACCORDING TO IRANIAN SEISMIC CODE

A. Gholizad*, H. Safari
Department of Engineering, University of Mohaghegh Ardabili, P.O. Box 56199-11367, Ardabil, Iran

Received: 5 March 2014; **Accepted:** 7 June 2014

ABSTRACT

The uncertain nature of future ground motions is leading to development of probabilistic structural damage estimation procedures. Fragility curves are useful tools for showing the probability of structural damage due to earthquakes as a function of ground motion indices. The contribution of this study is to develop the fragility curves for mid-rise RC frames designed according to the Iranian Seismic Design Code. These structures constitute the most vulnerable construction type in Iran well as several other countries prone to earthquakes. Sample 4, 6 and 8 story buildings were designed according to the Iranian seismic code. Incremental nonlinear dynamic analyses were performed for these sample buildings using ten near-fault ground motions to determine the maximum inter-story drift ratio. Based on those ratio fragility curves were developed in terms of peak ground acceleration for immediate occupancy and life safety damage levels with lognormal distribution assumption. The results show that sample frame structures do not satisfy performance objectives of Standard No. 2800.

Keywords: Fragility curves; Mid-Rise RC frames; incremental nonlinear dynamic analyses; damage levels.

1. INTRODUCTION

Mid-rise RC frame buildings constitute the major part of the building stock in Iran generally occupied for residential and commercial purposes. The damage to buildings from recent earthquakes and considering the fact that most of the metropolitan cities in Iran with highly dense population are located in high-risk seismic regions, close to active faults and knowledge of the significant effects of these earthquakes accompanied with a high death toll, point out the importance of risk assessment of existing building stock to estimate the potential damage from future earthquakes. For this purpose, fragility curves are useful tools,

*E-mail address of the corresponding author: *Gholizad@uma.ac.ir* (A. Gholizad)

since they allow estimation of the probability of exceeding a damage limit state due to earthquakes as a function of ground motion indices or various design parameters, for example: peak ground acceleration (PGA), elastic pseudo spectral acceleration (S_a), and elastic spectral displacement (S_d).

In the last fifteen years, a large number of researches have been carried out on the production of seismic fragility curves for RC buildings. Akkar et al. presented vulnerability curves for low-rise and mid-rise infilled frame RC buildings located in Duzce [1]. Rossetto and Elnashai produced vulnerability curves for low-rise RC frames, designed with the Italian seismic code [2]. Kircil and Polat developed the fragility curves for existing mid-rise RC frame buildings in Istanbul, which were designed according to the 1975 version of Turkey seismic design code [3]. Erberik developed fragility curves for typical low-rise and mid-rise RC buildings in Turkey [4]. Ozel and Guneyisi used fragility analysis as a tool to assess retrofitting effectiveness of a six-storey RC building using different types of eccentric steel braces on the seismic performance [5]. Ibrahim and El-Shami developed seismic fragility curves for mid-rise reinforced concrete frames in Kingdom of Saudi Arabia [6] Jeong et al. conducted fragility analyses to evaluate the relative seismic safety margins of seismic code-designed multi-story RC buildings with varying input motion intensity, ductility level and configuration [7].

The damage limit states in fragilities may be defined as global drift ratio (maximum roof drift normalized by the building height), inter-story drift ratio (maximum lateral displacement between two consecutive stories normalized by the story height), story shear force, etc. Inter-story drift ratio is considered in the present study as a measure of structural demands because it can be related to performance levels of reinforced concrete buildings in various seismic guidelines and in research performed by other investigators [1-7]. The purpose of Iranian Seismic Design code (Standard No. 2800) is to provide minimum provisions and regulations for the design and construction of buildings to resist the earthquakes effects. By these provisions, it is expected that in major seismic ground motions the loss of life is minimized while the stability of the buildings is maintained (Life Safety) and in low seismic ground motions the buildings shall maintain their operational level without major structural damage (Immediate Occupancy) [8]. FEMA 356 provided typical values of inter-story drift ratios for different structural systems for various structural performance levels. For concrete frames, the values are 1% and 2% for immediate occupancy (IO) and life safety (LS) levels [9].

Modeled structures were four, six and eight storey moment-resisting frames which were designed according to the 2005 version of Iranian Seismic Design Code. Incremental nonlinear dynamic analysis was performed under 10 near-fault ground motions to determine the inter-story drift ratios of sample buildings in terms of PGA. Two-parameter lognormal distribution is assumed for fragility curve construction, as was done traditionally in previous mentioned studies and a set of fragility curves was developed in terms of PGA. Such curves can be utilized in decision-making, disaster response planning and when considering the modification of local and regional building codes.

2. MODELS DESCRIPTION

Here, three samples of 4, 6 and 8 story RC moment resisting frames are considered with story height of 3 meters and bay width of 5 meters were assumed in accordance with the common practice. The lateral seismic forces affecting on structures were calculated using the equivalent lateral force. The structures were designed according to the 2005 version of Iranian Seismic Design Code under the effect of dead, live and seismic loads.

Figure 1 illustrates the typical frame of sample buildings, while Table 1 depicts beams and columns dimensions and reinforcement.

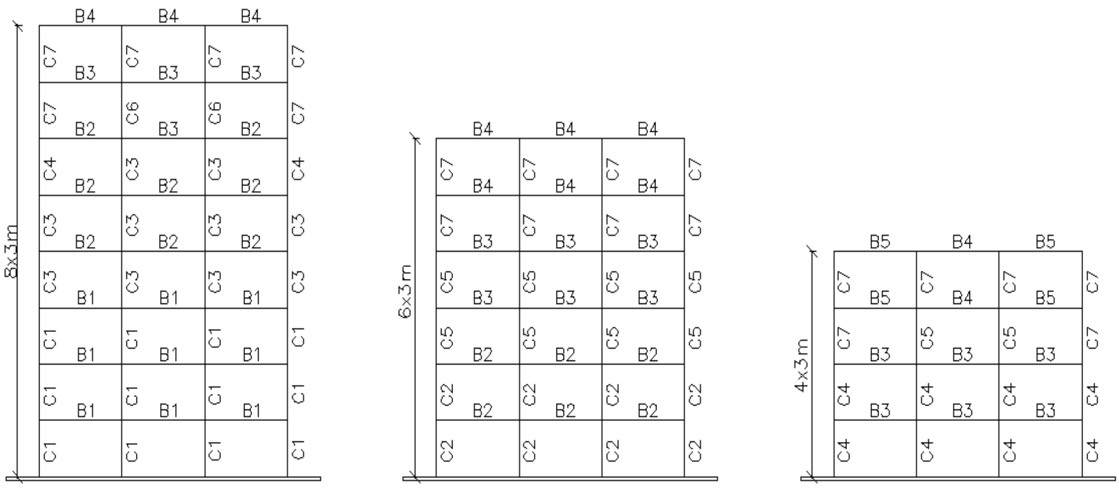

Figure 1. The typical frame of sample buildings

The soil type was assumed II, which is stiff soil with shear wave velocity (V_S) ranging from 375 to 750 m/s. The structures are classified as Moderate Importance, with importance factor I=1 and located in Zone 1, very high level of relative seismic hazard zone, with design base acceleration of 0.35g. For intermediate moment-resisting frames, the seismic response modification coefficient, R, is taken equal to 7.

The infill and partition walls were not considered as load carrying members. The natural period of the four, six and eight-story structures are 0.451 s, 0.611 s and 0.759 s respectively.

Table 1: Cross section of beams and columns

	Columns						
	C1	C2	C3	C4	C5	C6	C7
Dimensions (cm)	60×60	60×60	50×50	50×50	50×50	40×40	40×40
Reinforcement (mm)	16Φ25	16Φ20	16Φ22	16Φ20	16Φ18	16Φ20	12Φ16
	Beams						
		B1	B2	B3	B4	B5	
Dimensions (cm)		50×50	50×40	40×40	40×40	40×30	
Reinforcement (mm)		8Φ22	8Φ20	8Φ18	8Φ16	6Φ16	

For the nonlinear dynamic analysis of the sample buildings, materials strength was determined by their nonlinear properties.

For concrete material properties, the uniaxial nonlinear constant confinement model, initially programmed by Madas [15], that follows the constitutive relationship proposed by Mander et al. [16] and the cyclic rules proposed by Martinez-Rueda and Elnashai [17] was employed in SeismoStruct. The confinement effects provided by the lateral transverse reinforcement are incorporated through the rules proposed by Mander et al. [16] whereby constant confining pressure is assumed throughout the entire stress-strain range.

Four parameters need to be defined in order to fully characterize the concrete stress-strain curve. In the sample buildings the Ultimate compressive strength of concrete was 30 MPa, Strain at peak stress 0.002 m/m, confinement factor 1.09 and the specific weight 24 KN/m^3. The concrete material stress-strain curve is illustrated in the Figure 2 according to the specified properties.

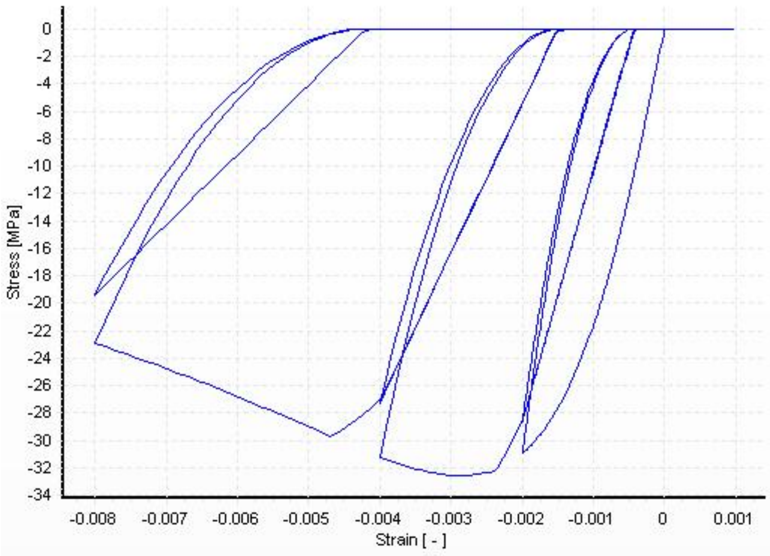

Figure 2. The concrete material stress-strain curve

For reinforcement steel material properties, the uniaxial bilinear stress-strain model with kinematic strain hardening, whereby the elastic range remains constant throughout the various loading stages and the kinematic hardening rule for the yield surface assumed as a linear function of the increment of plastic strain was employed in SeismoStruct. This simple model is also characterized by easily identifiable calibrating parameters and by its computational efficiency. It can be used in the modeling of both steel structures, where mild steel is usually employed, as well as reinforced concrete models, where worked steel is commonly utilized.

Five parameters need to be defined in order to fully characterize the reinforcement steel material stress-strain curve. In the sample buildings the Modulus of elasticity was 210 GPa, yield strength 400 MPa, strain hardening parameter 0.005, fracture/buckling strain 0.1 and specific weight 78 KN/m^3. The reinforcement steel material stress-strain curve is illustrated in the Figure 3 according to the specified properties.

Nonlinear flexural characteristics of the individual frame members were defined by moment-rotation relationships of plastic hinges assigned at the member ends. Flexural moment capacities were based on the section and material properties of members. Column capacities were calculated from the three-dimensional axial force-bending moment interaction diagrams.

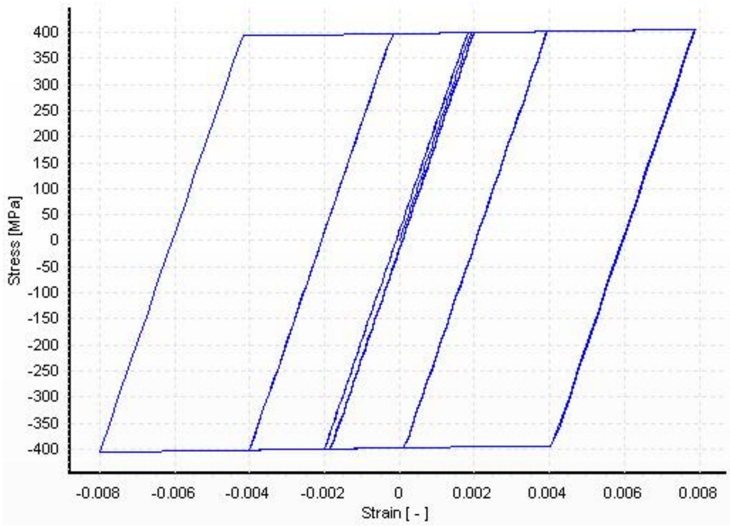

Figure 3. The reinforcement steel material stress-strain curve

A typical moment-rotation hinge backbone for frame members is shown in Figure 4. The segment OA, representing initial linear behavior, is followed by the post-yield behavior AB. Point B corresponds to the critical strength, where a sudden loss of strength occurs when the associated plastic rotation level is exceeded. The drop from B to C represents the initiation of failure in the member and D is the ultimate strength of the hinge.

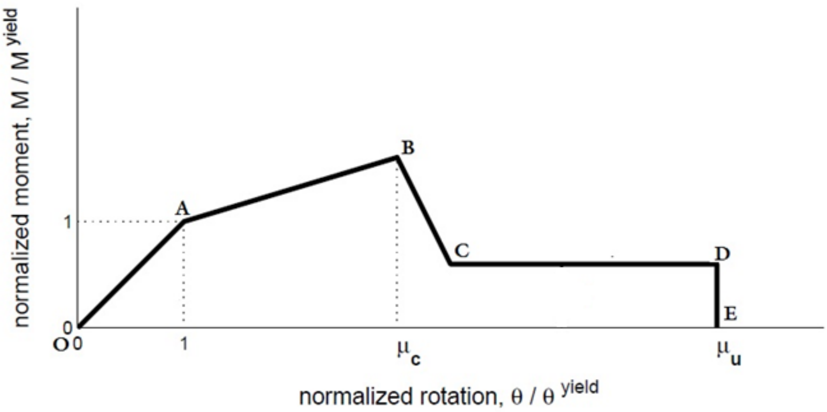

Figure 4. Normalized moment-rotation hinge backbone of a frame member-end

The plastic-hinge counterpart to the infrmFB element in SeismoStruct features a similar distributed inelasticity forced-based formulation, but concentrating such inelasticity within a fixed length of the element, as proposed by Scott and Fenves [18].

The plastic hinge is introduced as the polygonal hysteresis loop in SeismoStruct, as described in the work of Sivaselvan and Reinhorn [19]. The model can simulate the deteriorating behavior of strength, stiffness, and bond slip. Sixteen parameters need to be defined in order to fully characterize this response curve. The related parameters to backbone curve and hysteretic loops were derived from previous study on RC frames plastic hinges by A. Issa [20]. The structural model also includes P-Δ while the internal gravity frames have been directly incorporated.

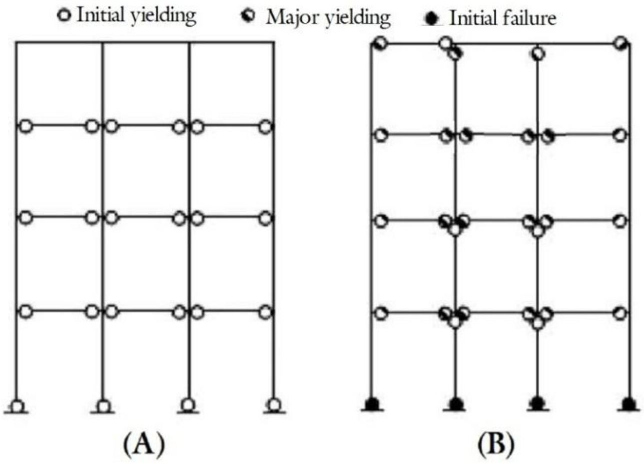

Figure 5. Plastic hinge patterns for the selected 4 story sample frame: A. status at yield capacity, and B. status at ultimate capacity

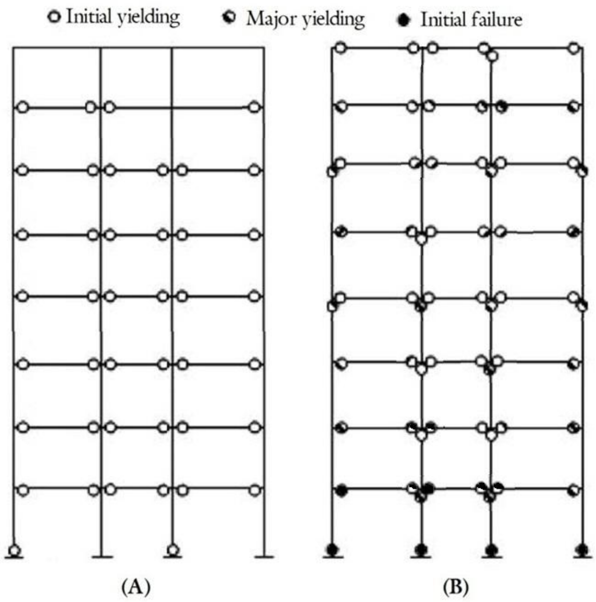

Figure 6. Plastic hinge patterns for the selected 8 story sample Frame: A. status at yield capacity, and B. status at ultimate capacity

It may be observed from Figures 5 and 6 that the damage sequence in both frames starts with the yielding of beam ends at the lower stories, which further propagates to upper stories, and finally with the yielding of column bases. This is an expected sequence in achieving a ductile beam mechanism.

3. GROUND MOTIONS

The random nature of earthquakes makes the damage estimation problem probabilistic. Shome and Cornell [11] have shown that, for mid-rise buildings, ten to twenty ground motion records are usually enough to provide sufficient accuracy in the estimation of seismic demand. Ten near-fault ground motions have been used in this study to take the random nature of earthquakes into consideration. Table.2 indicates the properties of applied ground motions. The records were generally recorded on stiff-to-medium sites.

Table 2: Details of ground motions

No.	Ground motion	Location	Station	Year	Mw	Distance from fault rupture (km)	PGA (g)
1	Manjil	Iran	Abbar	1990	7.3	10.0	0.536
2	Bam	Iran	Bam	2003	6.5	1.0	0.771
3	Tabas	Iran	Tabas	1978	7.4	1.2	0.83
4	Ahar-Varzeghan	Iran	Sattarkhan Dam	2012	6.2	1.3	0.487
5	Erzincan	Turkey	Erzincan	1992	6.9	2.0	0.40
6	Northridge	USA	LA Dam	1994	6.7	2.6	0.34
7	Kobe	Japan	Nishi-Akashi	1995	6.9	11.1	0.50
8	Chi-Chi	Taiwan	CHY028	1999	7.6	2.3	0.65
9	Duzce	Turkey	Duzce	1999	7.1	8.3	0.53
10	Morgan Hill	USA	Halls Valley	1984	6.2	3.4	0.15

The closest distance to fault was between 1-15 km. Near-fault ground motions, which caused much of the damage in recent major earthquakes (Northridge 1994, Kobe 1995, Chi-Chi 1999), are characterized by a pulse-like motion that exposes the structure to high input energy at the beginning of the record.

Iran is located at a zone which has a prone to having strong earthquakes and nearly in the majority of the country quake risk exists, also, several near-fault earthquakes with extensive damages were occurred in Iran (Tabas 1987, Bam 2003, Ahar-Varzeghan 2012). Since High statistics of damages in buildings structured based on codes exposed to near-fault earthquakes and because in Iranian seismic code there is no considerations for designing buildings at Near-fault regions, seismic risk analysis of buildings designed according to Iranian seismic code and subjected to this kind of earthquakes is important for identifying the seismic vulnerability of structural systems under the effect of potential strong ground motions.

4. DAMAGE LEVELS

Damage levels were considered in accordance with FEMA356 and maximum inter-story drift ratio was accepted as the damage measure. For concrete frames, inter-story drift ratio limits are 0.01 and 0.02 for IO and LS levels, as explained in the following.

- Immediate Occupancy (IO): The building experiences minimal or no damage to the structural elements and only minor damage to the non-structural components. Immediate occupancy may be possible. However, some clean-up, repair and restoration of service utilities may be necessary before the building can function as before earthquake.
- Life Safety (LS): The structural and non-structural components are subjected to extensive damage and are in need of repairs before re-occupancy. Repair is possible but may be economically impractical.

5. INCREMENTAL NONLINEAR DYNAMIC ANALYSIS

Incremental nonlinear dynamic analysis (IDA) is a parametric analysis method that is useful for estimating structural performance under several ground motions [12]. It mainly involves producing one or more curves of damage measure versus intensity measure under the effect of scaled ground motions as a result of several non-linear dynamic analyses. These ground motions can be selected from real records of earthquakes or can be generated artificially. Real records are more realistic since they include all ground motions characteristics such as amplitude, frequency, duration, energy content, number of cycles and phase [13]. For this study, the maximum inter-story drift ratio is assumed as the best damage indicator and peak ground acceleration (PGA) is selected as the ground motion intensity measure. Under each ground motion, nonlinear time history analyses were conducted while scaling the PGA, of chosen ground motion incrementally every 0.05g, until structural instability is obtained or up to PGA 0.8g. The SeismoStruct computer program [14] was utilized for non-linear dynamic analysis and the maximum inter-story drift ratio is recorded at the end of each analysis. The relationship between the maximum inter-story drift ratio and the corresponding PGA was obtained, which creates the IDA curves for a certain structure under the specified ground motion. The IDA curves of sample frames are shown in Figure 7.

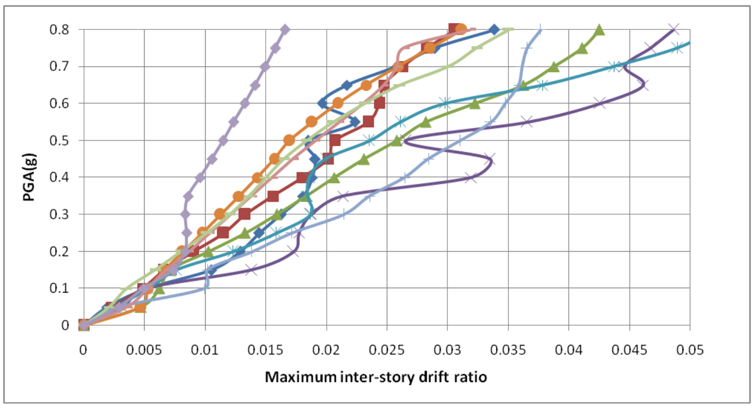

(a)

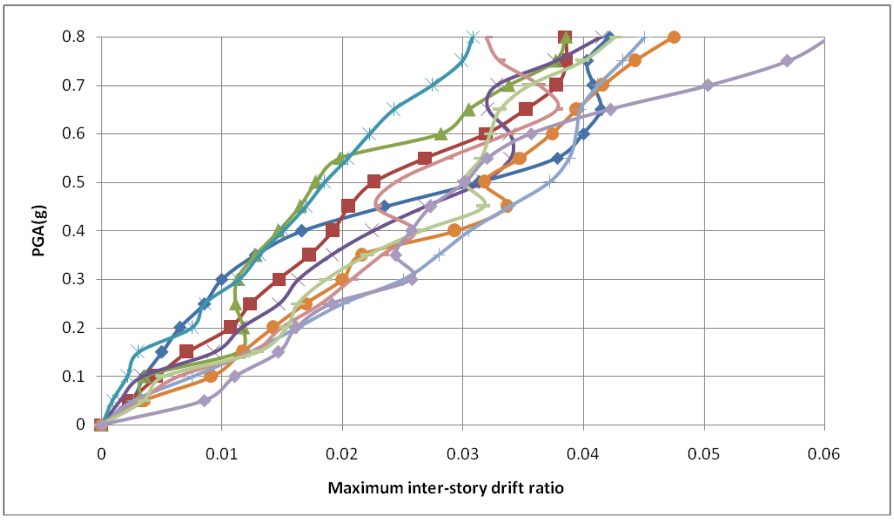

(b)

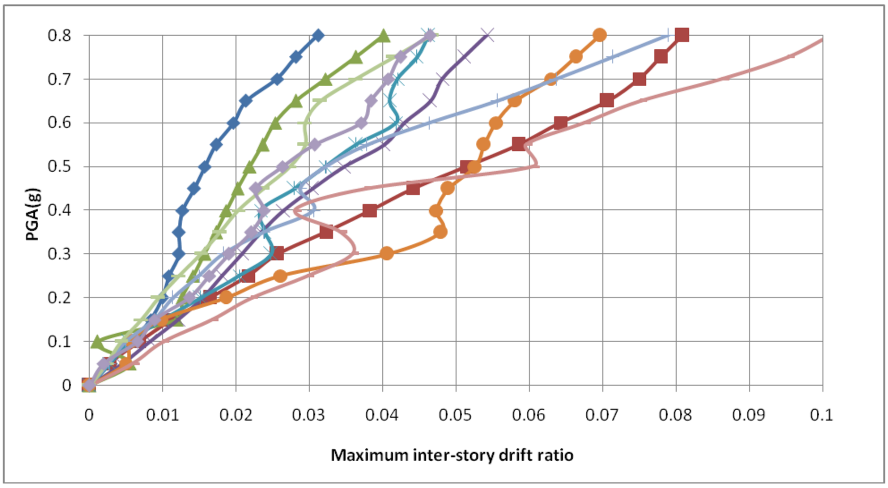

(c)

Figure 7. IDA curves generated for (a) 4-story, (b) 6-story and (c) 8-story sample frames under selected ten ground motions

6. FRAGILITY CURVES

Fragility curves express the probability of structural damage due to earthquakes as a function of ground motion indices. In this study, fragility curves were constructed in terms PGA. It is assumed that the fragility curves can be expressed in the form of two-parameter lognormal distribution functions. Based on this assumption, the cumulative probability of the occurrence of damage, equal to or higher than damage level D, is defined by:

$$P(\leq \mathrm{D}) = \Phi\left(\frac{\ln X - \lambda}{\xi}\right) \tag{1}$$

Where Φ is the standard normal distribution, X is the lognormal distributed ground motion index (PGA), and λ and ξ are the mean and standard deviation of ln(X). The mean and standard deviation of ground motion indices for each damage level are obtained, as shown in Figure 8, which is a lognormal plot of ln(X) and the corresponding standard normal variable. This method is based on plotting ln(X) versus the corresponding standard normal variable on a lognormal scale and performing a linear regression analysis to determine the mean and standard deviation of ln(X) for each damage level. The relationship between the standard normal variable and the mean and standard deviation of ln(X) can be expressed as:

$$s = \frac{\ln X - \lambda}{\xi} \tag{2}$$

Where s is the standard normal variable. Figure 8 shows the typical lognormal probability plot for the LS damage level of sample 8 story frame.

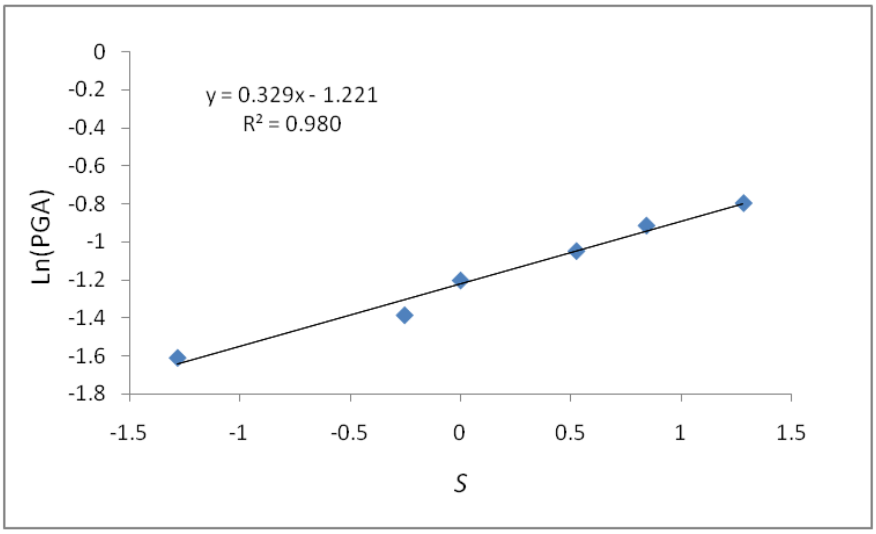

Figure 8. Lognormal probability plot for LS probability curve of 8-story frame

Table 3 shows the mean and standard deviation of lognormal distributed PGA for each sample building and damage level under consideration. Fragility curves of sample frames in terms of PGA are shown in Figure 9.

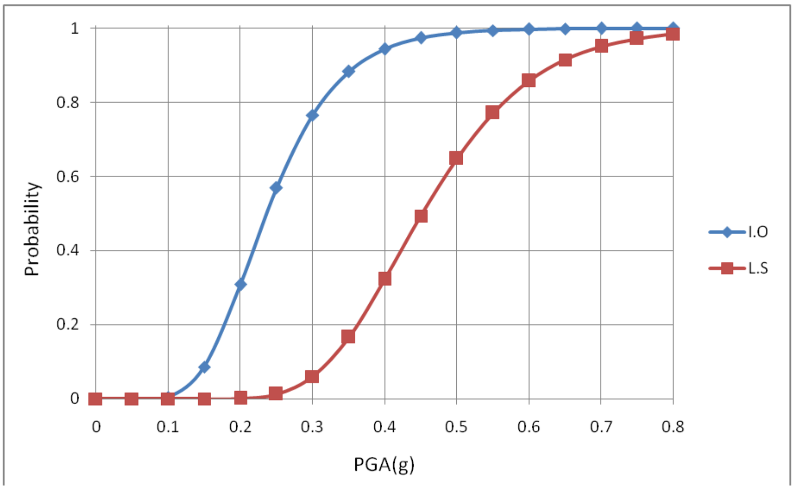

(a)

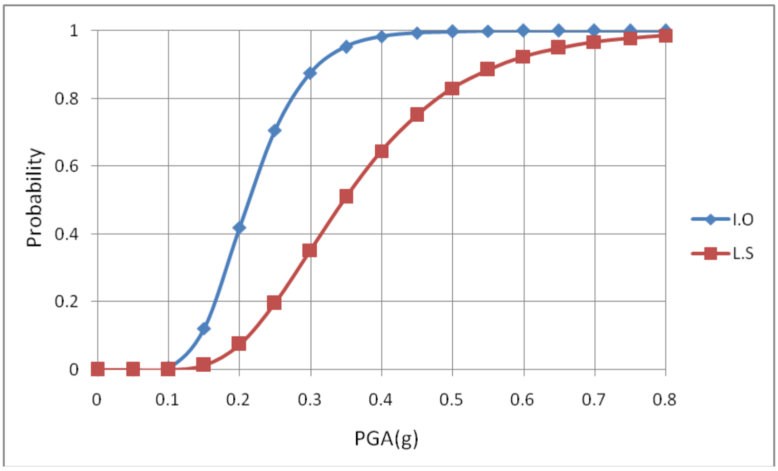

(b)

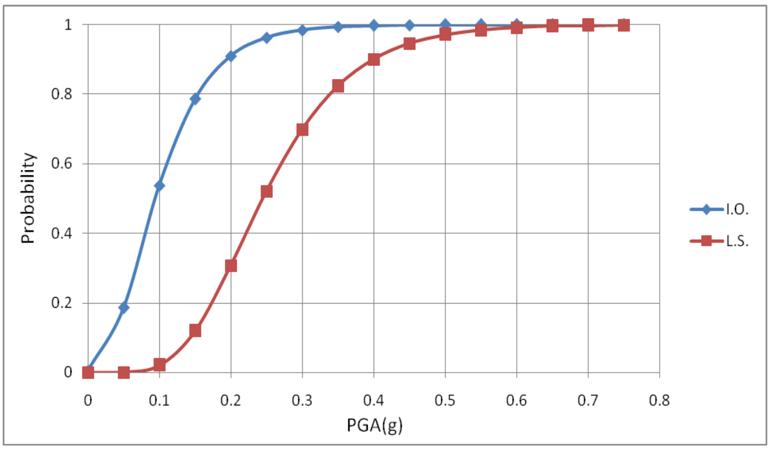

(c)

Figure 9. Fragility curves of (a) 4-story, (b) 6-story and (c) 8-story sample frames

Table 3: Parameters of lognormal distributed PGA

	IO		LS	
Number of story	ξ	λ	ξ	λ
4-story	0.363	-1.669	0.264	-0.794
6-story	0.429	-1.819	0.384	-1.059
8-story	0.411	-1.936	0.329	-1.221

7. CONCLUSION

In Iranian Seismic Design Code, the goal of the design is Life Safety performance under major seismic ground motions and Immediate Occupancy performance under moderate and low seismic ground motions. Major seismic ground motion or “Design Level Earthquake” is the ground motion with a 10 percent probability of not being exceeded in 50 years. Low and moderate seismic ground motions or “Service Level Earthquake” is the ground motion that has a 99.5 percent probability of not being exceeded in 50 years. The ground motion characteristic for Service Level Earthquake shall be similar to the design base earthquake, except that the design base acceleration ratio, shall be reduced by a factor of 6 [8]. The Peak Ground Acceleration of Design Level Earthquake and Service Level Earthquake for high risk seismic zones of Iran are 0.35g and 0.35g/6.

The fragility values of Immediate Occupancy performance level at PGA of 0.35g/6 are 0% for three sample frames, and these values for life safety performance level corresponding to the design base PGA (0.35g) for the 4, 6 and 8 story buildings are 17%, 51% and 70% respectively. The results show that sample structures exceed the Life Safety (LS) limit state under the design PGA. This pattern is so dramatic for 8-story frame buildings with 70% probability of exceeding. Therefore, mid-rise RC frame structures designed according to Iranian Standard No. 2800 do not satisfy performance objectives of this code.

REFERENCES

1. Akkar S, Sucuoglu H, Yakut A. Displacement-based fragility functions for low- and mid-rise ordinary concrete buildings, *Earthquake Spectra*, No. 4, **21**(2005) 901-27.
2. Rossetto T, Elnashai A. A new analytical procedure for the derivation of displacement-based vulnerability curves for populations of RC structures, *Engineering Structures*, No. 3, **27**(2005) 397-409.
3. Kircil MS, Polat Z. Fragility Analysis of Mid-Rise R/C Frame Buildings, *Engineering Structures*, No. 9, **28**(2006) 1335-45.
4. Erberik MA. Fragility-based assessment of typical mid-rise and low-rise RC buildings in Turkey, *Engineering Structures*, No. 5, **30**(2008) 1360-74.
5. Ozel AE, Guneyisi EM. Effects of eccentric steel bracing systems on seismic fragility curves of mid-rise R/C buildings: a case study, *Structural Safety*, No. 1, **33**(2011) 82-95.
6. Ibrahim YE, El-Shami MM. Seismic fragility curves for mid-rise reinforced concrete frames in Kingdom of Saudi Arabia, *The IES Journal Part A: Civil & Structural*

Engineering, No. 4, **4**(2011) 213-23.
7. Jeong S, Mwafy AM, Elnashai AS. Probabilistic seismic performance assessment of code-compliant multi-story RC buildings, *Engineering Structures*, **34**(2012) 527-37.
8. *Iranian Code of Practice for Seismic Resistant Design of Buildings*, Standard No.2800, 3rd ed, Building and housing research center (BHRC), 2005.
9. FEMA 356. *Pre standard and commentary for the seismic rehabilitation of buildings*, Washington DC: Federal Emergency Management Agency, 2000.
10. Mander JB, Priestley MJN, Park R. Theoretical stress-strain model for confined concrete, *Journal of Structural Engineering*, No. 8, **114**(1988) 1804-26.
11. Shome N, Cornell CA. *Probabilistic Seismic Demand Analysis of nonlinear structures*, Ph.D. dissertation, Stanford University, 1999.
12. Vamvatsikos D, Cornell CA. Incremental dynamic analysis, *Journal of Earthquake Engineering and Structural Dynamics*, No. 3, **31**(2002) 491-514.
13. Rota M, Penna A, Magnes G. A methodology for deriving analytical fragility curves for masonry buildings based on stochastic nonlinear analyses, *Engineering Structures*, **32**(2010) 1312-3.
14. SeismoStruct Ver. 5.2.2. SeismoSoft, earthquake engineering software solutions [online]. Available from: www.seismosoft.com, 2013.
15. Madas P. *Advanced Modeling of Composite Frames Subjected to Earthquake Loading*, PhD Thesis, Imperial College, London, UK, 1993.
16. Mander JB, Priestley MJN, Park R. Theoretical stress-strain model for confined concrete, *Journal of Structural Engineering*, No. 8, **114**(1988) 1804-26.
17. Martinez-Rueda JE, Elnashai AS. Confined concrete model under cyclic load, *Materials and Structure*s, No. 197, **30**(1997) 139-47.
18. Scott MH, Fenves GL. Plastic hinge integration methods for force based beam–column elements, *ASCE Journal Of Structural Engineering*, No. 2, **132**(2006), 244-52.
19. Sivaselvan M, Reinhorn AM. *Hysteretic Models for Cyclic Behavior of Deteriorating Inelastic Structures*. Report MCEER-99-0018, MCEER/Buffalo, 1999.
20. Issa A, Filippou FC, D'Ambrisi A. *Nonlinear Static and Dynamic Analysis of Reinforced Concrete Subassemblage*, Ph.D. dissertation, University of California, Berkeley, 1992.